Journal of Physics: Conference Series

PAPER • **OPEN ACCESS**

Influence of the guide vanes design on stress parameters of Francis-99 turbine

To cite this article: M Lazarevikj *et al* 2019 *J. Phys.: Conf. Ser.* **1296** 012008

View the article online for updates and enhancements.

IOP ebooks™

Bringing you innovative digital publishing with leading voices to create your essential collection of books in STEM research.

Start exploring the collection - download the first chapter of every title for free.

This content was downloaded from IP address 95.180.201.66 on 24/08/2019 at 12:47

IOP Conf. Series: Journal of Physics: Conf. Series **1296** (2019) 012008 doi:10.1088/1742-6596/1296/1/012008

Influence of the guide vanes design on stress parameters of Francis-99 turbine

M Lazarevikj[1], F Stojkovski[1], I Iliev[2], Z Markov[1]

[1] "Ss. Cyril and Methodius" University in Skopje, Faculty of Mechanical Engineering-Skopje, Karpos II bb, 1000 Skopje, Republic of North Macedonia

[2] Waterpower Laboratory, Department of Energy and Process Engineering, Norwegian University of Science and Technology, Alfred Getz Vei 4, Trondheim, Norway

marija.lazarevikj@mf.edu.mk

Abstract. The frequencies with predominant amplitudes in low specific speed Francis turbines are related to rotor-stator interaction and they are calculated on the basis of the runner rotational speed and the number of guide vanes and runner blades. Pressure pulsations in the blade channels can be a reason for noise and vibration in the turbine above allowed level. High pressure pulsations can be caused by certain combination of runner blades and guide vanes number and/or resonance with one of the runner's natural frequencies. The stress parameters of the Francis-99 turbine guide vanes and their modifications are analysed in this paper. The main aim is to determine the impact of the geometry modification (thinner for increased efficiency) of the guide vanes on the Francis turbine stresses by performing numerical simulations. The original Francis-99 turbine guide vane geometry and three modifications consisting of new guide vane shapes are being considered. The numerical investigation of the flow field is based on the k-ω SST turbulence model with 'frozen rotor' approach selected, constituting a quasi-steady state analysis, without taking into account the physical rotation of the runner to obtain Rotor-Stator Interaction (RSI). Pressure distribution on one guide vane determined by a Computational Fluid Dynamics (CFD) simulation of the turbine is coupled to a Finite Element Method (FEM) simulation in order to analyse the stresses. The results from the one-way fluid-structure interaction analysis give the stresses distribution and deformations of the guide vanes. Moreover, modal-acoustics analysis is conducted to obtain the natural frequencies of the guide vanes in water and comparison is made with the calculated vortex shedding frequencies to estimate the risk of resonance.

Keywords: frequency, pressure distribution, FEM, Francis turbine

1. Introduction

Hydraulic turbines often operate at off-design conditions in order to fulfill the exact energy demand. The operation outside the best efficiency point causes higher dynamic loads and stresses over the turbine components and possible vibration problems. Such fluctuating loads can cause material failure [1]. Hence, knowledge of the mechanical response of the turbine elements at different operating conditions is essential [2].

Resonant behavior can result in severe load cases or failure, but it is most feared for fatigue problems [3]. Fatigue of materials occurs due to external fluctuating loads whose intensity affects the lifetime of turbine blades. However, the frequency of the excitation force is at least as important as its magnitude.

Content from this work may be used under the terms of the Creative Commons Attribution 3.0 licence. Any further distribution of this work must maintain attribution to the author(s) and the title of the work, journal citation and DOI.
Published under licence by IOP Publishing Ltd

Therefore, detailed knowledge of the expected frequencies of the excitation forces and the natural frequencies of the structure becomes vital in order to prevent problems with resonance and fatigue of turbine elements as structures subjected to dynamic loads [4]. This imposes solving two problems of structural dynamics - determining natural frequencies and corresponding mode shapes and their comparison with the frequencies of excitation, on one hand, and conducting a time dependent analysis of structure motion under loads, on the other hand [5].

2. Theoretical background

Guide vanes cascades in hydraulic turbines undergo fluid-structure coupling phenomena. Fluid-structure interaction (FSI) can be described by the coupling of the equation of motion of the structure:

$$m_s \cdot \ddot{x} + d_s \cdot \dot{x} + k_s \cdot x = F(t) \tag{1}$$

where m_s is the structural mass, d_s is the structural damping, k_s is the structural stiffness, F is the applied load vector and x is the nodal displacement;
and the equation of fluid flow:

$$\rho(\frac{\partial v}{\partial t} + v \cdot \nabla v) = -\nabla p + \nabla \cdot T + f \tag{2}$$

where ρ is the fluid density, $v \cdot \nabla v$ is the flow velocity vector, p is the pressure, T is the deviatoric stress tensor and f is body forces per unit volume acting on the fluid [6]. The equation for the conservation of mass is:

$$\frac{\partial \rho}{\partial t} + \nabla \cdot (\rho v) = 0 \tag{3}$$

For incompressible fluid, the Navier-Stokes equations can be written as:

$$\rho(\frac{\partial v}{\partial t} + v \cdot \nabla v) = -\nabla p + \mu \nabla^2 v + f \tag{4}$$

where $\partial v / \partial t$ is the unsteady acceleration term, $v \cdot \nabla v$ is the convective acceleration term, $-\nabla p$ is the pressure gradient and μ is the fluid dynamic viscosity. The equation of mass conservation can be reduced to:

$$\nabla \cdot v = 0 \tag{5}$$

The understanding of the fluid-structure coupling in the guide vanes cascade imposes the knowledge of dynamic behaviour of the blades [7]. Dynamic fluid flow effects depend on the operating conditions and specific speed of Francis turbines and can cause pressure oscillations in hydraulic turbines.

Pressure fluctuations in hydraulic machinery are influenced by machine design, operating conditions and by the dynamic response of the water conduits and rotating components [8]. At full load operation of low specific speed turbines, the interaction between the rotating runner and stationary guide vanes known as Rotor-Stator Interaction (RSI) is dominant. At part load, draft tube oscillations are influenced by the rotating vortex rope, whereas at deep part load, channel vortices in the runner can be a reason for pressure fluctuations [9].

Reason for a failure in Francis turbines can be a resonance of the runner with the pressure field from the guide vanes. The pressure from the rotating runner causes pressure fluctuations in the vaneless space, guide vane cascade and upstream in the spiral casing and inlet conduit [10]. This interaction of the rotor and stator produces an oscillating pressure field [11]. The source of fluctuations is the downstream runner with high and low pressure sides of the blades giving fluctuations in the downstream boundary condition of each guide vane passage, and also, the interaction between the wicket gates wake with the runner blades [10, 11, 12]. On the one hand, the rotating observer passes the wakes of all guide vanes during a full rotation, and on the other hand, a pressure pulse is induced each time when a runner blade is passing a guide vane [13].

The pressure oscillations are related to flow velocity disturbances and unsteady pressure field when passing one runner blade in front of one guide vane which means they are associated with the blade passing frequency and guide vane frequency [8].

The guide vanes will be subject to a time varying pressure field due to the passing of the runner blades. This pressure field will oscillate with the runner rotational frequency [12]:

$$f_n = \frac{n}{60} \tag{6}$$

where n is the runner rotational speed in [rev/min].

The runner blade passing frequency f_{BP} is calculated as:

$$f_{BP} = f_n \cdot z_r \tag{7}$$

where z_r is the number of runner blades.

The vortex shedding frequency f_{Sh} of the guide vane can be estimated from the Strouhal number S_h [14]:

$$f_{Sh} = S_h \cdot \frac{v}{t_{edge}} \tag{8}$$

where t_{edge} is the guide vane trailing edge thickness and v is the undisturbed free-stream flow velocity near the trailing edge [15].

Estimating the risk of resonance and potential blade cracking includes assuming a Strouhal number in the range of $0.18 \div 0.25$, calculating the frequency and its correlation with the natural frequencies [16]. Natural frequencies are governed by structural and acoustic properties [17]. Regarding the strong influence on the turbine structure elements by their confinement in water [18,19], natural frequencies decrease due to the added mass of the surrounding water [20].

Neglecting the structural damping, equation (1) gets the following form:

$$m_s \cdot \ddot{x} + k_s \cdot x = F(t) \tag{9}$$

For free vibration, combining equation (9) with the fundamental equation of simple harmonic motion:

$$\ddot{x} + \omega_n^2 x = 0 \tag{10}$$

the natural frequency of the first bending mode of the guide vane structure can be obtained as:

$$f_{n1} = \frac{1}{2\pi}\sqrt{\frac{k_s}{m_s}} \tag{11}$$

The basic equation of motion governing torsional oscillation with damping is:

$$J_\theta \ddot{\theta} + 2J_\theta \xi_\theta \dot{\theta} + k_\theta \theta = F(t) \tag{12}$$

where $F(t)$ is the external excitation, k_θ represents the stiffness of the guide vane material, ξ_θ is a damping coefficient and J_θ denotes the torsional moment of inertia of the guide vane.

Neglecting the damping, for a free-vibration system, equation (12) gets the following form:

$$J_\theta \ddot{\theta} + k_\theta \theta = 0 \tag{13}$$

Using equation (13) and the fundamental equation of simple harmonic motion:

$$\ddot{\theta} + \omega_n^2 \theta = 0 \tag{14}$$

the natural frequency of the first torsional mode of the guide vane structure can be obtained as:

$$f_n = \frac{\omega}{2\pi} = \frac{1}{2\pi}\sqrt{\frac{k_\theta}{J_\theta}} \tag{15}$$

From torsion equation, the value of the stiffness is:

$$k_\theta = \frac{GI}{l} \tag{16}$$

where G is modulus of rigidity of guide vane material, I is the polar moment of inertia of the guide vane and l is its length (height).

For prediction of the dynamic characteristics of the guide vanes when submerged in water, the effect of the water that surrounds must be taken into account. The most accurate way to calculate the natural frequency of guide vane in water is to perform a modal acoustics analysis where the guide vane is submerged in water.

3. Numerical setup

Based on the existing design of the Francis-99 guide vanes, a similar guide vane shape was designed, with minor differences in the inlet and outlet angle, the vane tail shape and the location of the maximal thickness as shown on figure 1. Using the theory of 4 digit NACA airfoils, non-standard airfoil shape 'NACA 3320' is created.

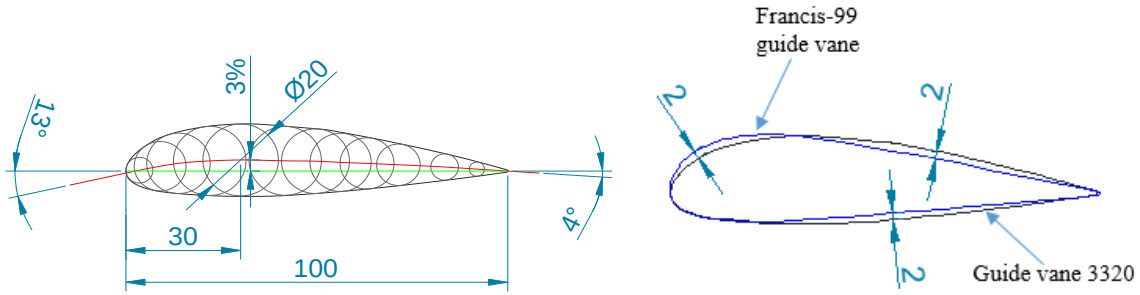

Figure 1. NACA 3320 (left) and its geometry discounts compared to Francis-99 guide vanes (right)

Three 3D numerical models were built and simulations were conducted using ANSYS Software. The models consist of the original spiral casing, stay vanes, runner and draft tube from model Francis-99 and include different guide vanes shape.

The first model was noted as NACA 3320 with 20% thickness of the blade. The other two models are tested with reduced thickness of the blade to 18% and 16% in order to see the influence of the thickness.

The models are tested for four different operating conditions marked as part load 1 (PL-1), part load 2 (PL-2), best efficiency point (BEP) and high load (HL) that correspond to guide vane angle of 6.72°; 3.91°; 9.84° and 12.43° according to the Francis-99 reports [21, 22]. All CFD models are calculated for equal guide vane passage (a=const., Re=const) at same operating regimes, so that the models can be comparable.

For modelling turbulent flow in the hydraulic turbine, k-ω SST turbulence model with 'frozen rotor' approach is selected. The runner rotational speed is 333 rpm. Boundary conditions in the numerical model are mass flow inlet at the spiral casing inlet and pressure outlet at the draft tube outlet, with values taken from the Francis-99 reports for the respective operating conditions (figure 2).

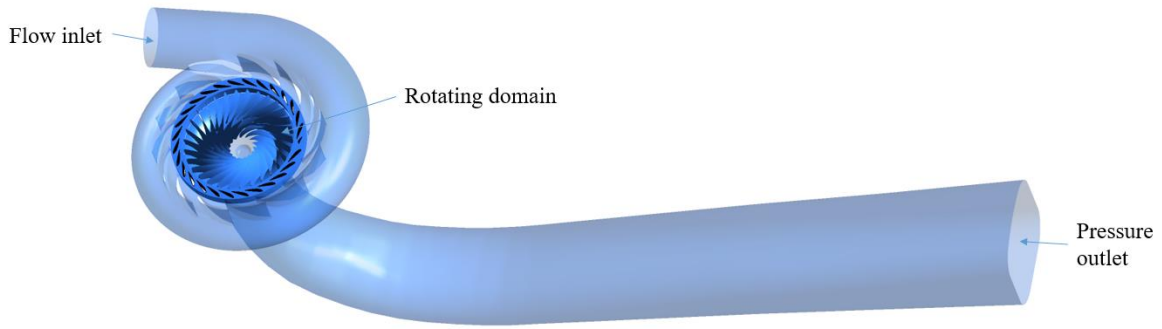

Figure 2. Fluid domain and boundary condition

The fluid flow simulations are then coupled to static structural simulation (one-way FSI) and steady FEM analysis is performed to evaluate the overall loads and the highest stresses on the guide vanes, using ANSYS Mechanical. One guide vane (figure 3) is chosen for analysis.

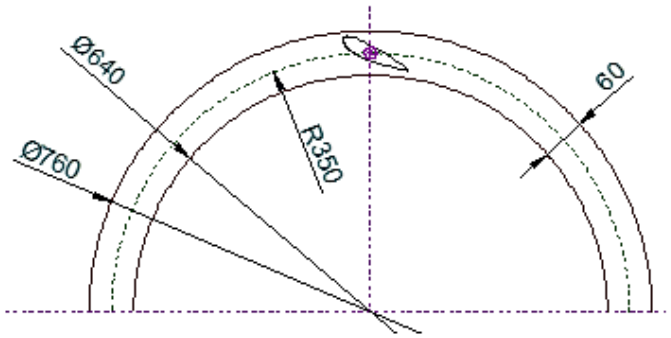

Figure 3. Location of guide vane analysed

Unstructured tetrahedral mesh which consists of approximately 23440 elements is generated for the structural domain (figure 4). The pressure distribution obtained from the steady state simulations of the fluid flow in the turbine is applied to the guide vanes surfaces of the finite element model. The procedure includes interpolation between the meshes of the fluid domain and the solid domain.

Cylindrical support boundary condition is used for the guide vane shaft. The shaft passes through the guide vane centroid. The dimension of the shaft is arbitrarily chosen, only to serve as support. The material for the guide vanes is stainless steel with modulus of elasticity $E = 1.93 \cdot 10^5 [MPa]$, density $\rho_{material} = 7900[kg/m^3]$ and Poisson ratio of $\nu = 0.3$.

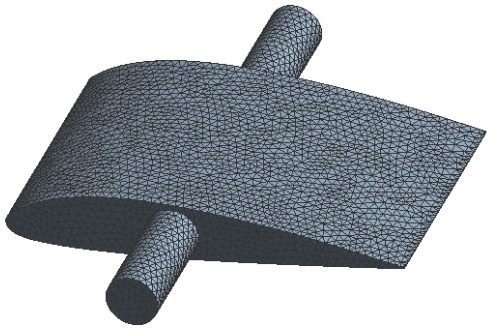

Figure 4. Numerical mesh of the guide vane

To obtain the natural frequencies and mode shapes of the selected guide vane, a FEM analysis of the guide vane, firstly surrounded by air and then by water was carried out. In order to make the complete model for the simulation in water, the guide vane defined as a structure was surrounded by acoustic-fluid domain with compatible dimension. The same set of nodes is shared by both domains on the interface. The generated mesh for both the modal analysis and modal-acoustics analysis is shown on figure 5.

The corresponding boundary condition at the interface between the guide vane and the water was a FSI interface so that the displacement of the structure is identical to that of the fluid in normal direction. Rigid wall boundary where the nodal displacement equals zero is set on the external water surfaces. The acoustic domain is specified with water liquid. Properties of water used at normal pressure and temperature were density of $\rho_{water} = 1000[kg/m^3]$ and sonic speed $c = 1483[m/s]$.

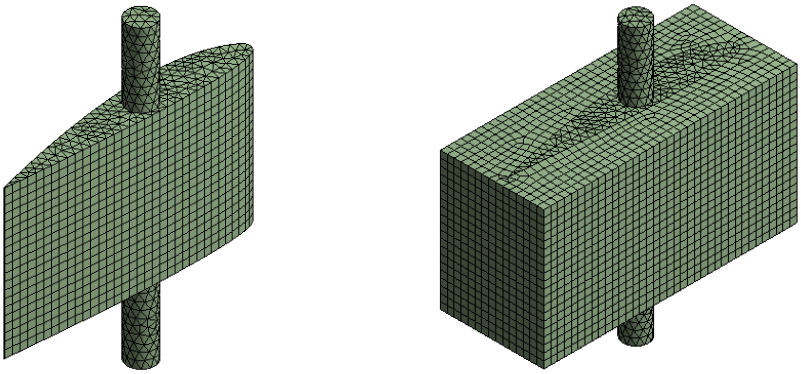

Figure 5. Numerical mesh for the modal and modal-acoustics analysis

4. Results

The analysis of the stress distribution and deformation of guide vanes show the influence of both the profile thickness and the operating regime.

The total deformation of the guide vanes 3316, 3318 and 3320 at part load 1, part load 2, best efficiency point and at high load, respectively, is shown on figure 6.

The maximum total deformation is found for the guide vane profile 3316 at the deep part load operation (blade passage of 5.1 mm) and its value is $4.5 \cdot 10^{-3}$ mm. The total deformation decreases with the thickness of the guide vane for the same operating regime. The deformation increases when going from high load to deep part load for every type of guide vane. The lowest total deformation of $7.12 \cdot 10^{-4}$ mm is seen on the guide vane with highest thickness – 3320 when the turbine operates at high load (blade passage of 18 mm). This can be observed on the graph shown on figure 7, where the maximum total deformation of each guide vane type is given at the respective operating conditions (deep part load, part load, best efficiency and high load).

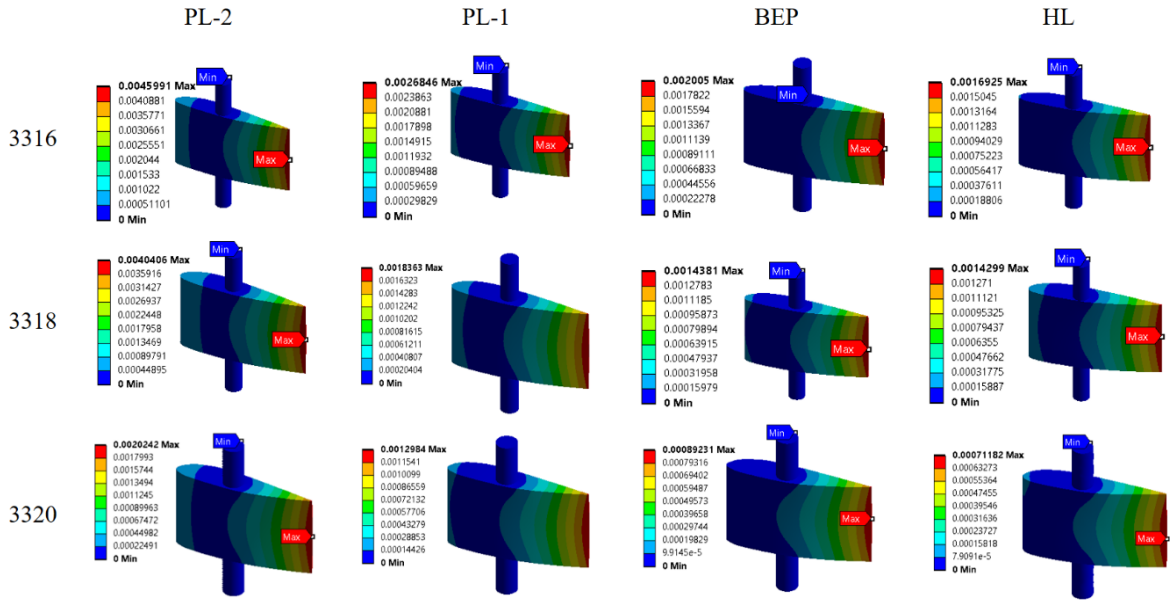

Figure 6. Total deformation of guide vanes 3316, 3318 and 3320 for the respective operating regimes

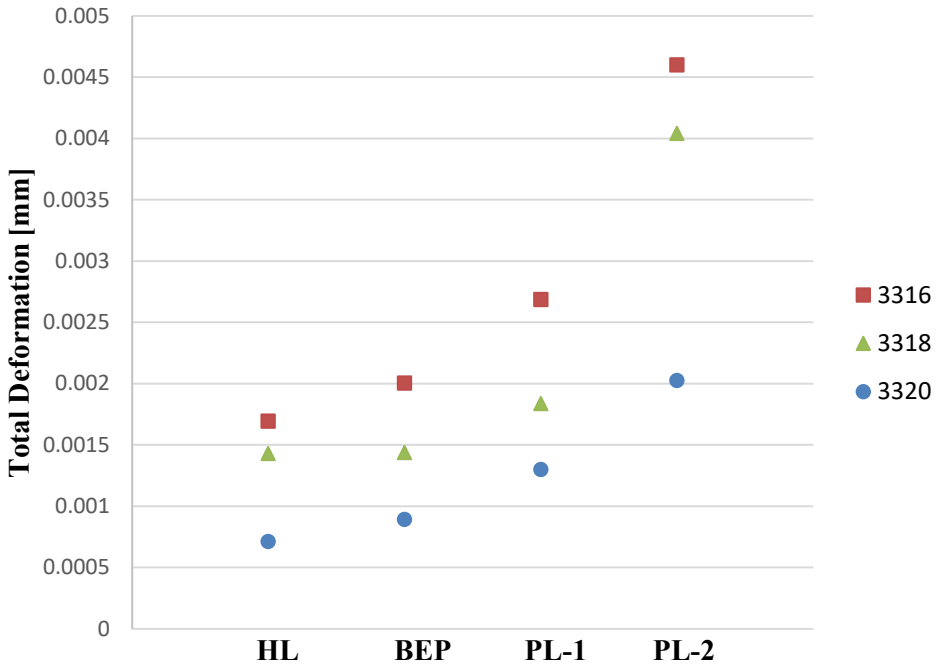

Figure 7. Maximum total deformation of guide vanes at different operating conditions

The distribution of the equivalent (Von-Mises) stress of the guide vanes with different thickness at all operating conditions analysed is shown on figure 8.

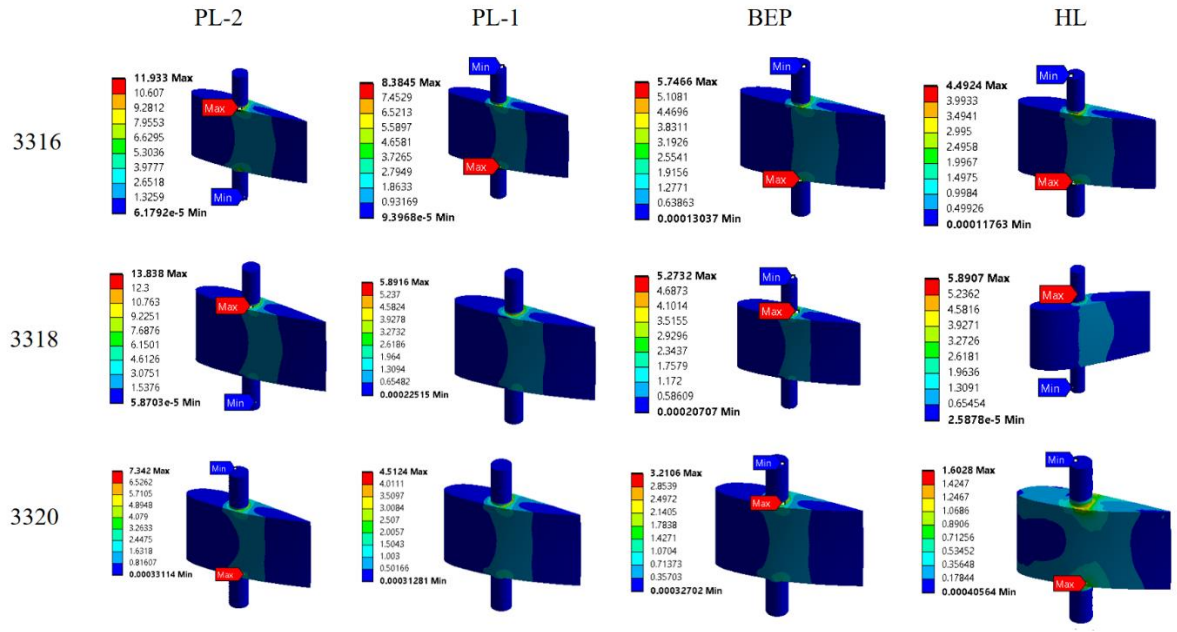

Figure 8. Equivalent (Von-Mises) stress distribution of guide vanes 3316, 3318 and 3320 for the respective operating regimes

The stress increases going from high load to deep part load operation for every type of profile. The stress magnitude is in the range from 4.5 to 12.9 [MPa], 5.9 to 13.8 [MPa] and 1.6 to 7.3 [MPa] for guide vane 3316, 3318 and 3320, respectively. The lowest value of the stress is found at guide vane 3320 at high load, whereas the highest value is noticed for guide vane 3318 at deep part load.

The blade passing frequency is calculated according to equation (7):

$$f_{BP} = 166.5[Hz]$$

Using equation (8), the vortex shedding frequencies of the guide vanes at different operating conditions are calculated. The values for guide vanes 3320, 3318 and 3316 are given in table 1, 2 and 3, respectively.

Table 1. Vortex shedding frequencies of guide vane 3320 at different operating conditions.

	3320			
	PL-2	**PL-1**	**BEP**	**HL**
Vortex shedding frequency [Hz]	395.6	785.3	1130.8	1378.7

Table 2. Vortex shedding frequencies of guide vane 3318 at different operating conditions.

	3318			
	PL-2	**PL-1**	**BEP**	**HL**
Vortex shedding frequency [Hz]	393.2	783.8	1096.7	1379.5

Table 3. Vortex shedding frequencies of guide vane 3316 at different operating conditions.

	3316			
	PL-2	**PL-1**	**BEP**	**HL**
Vortex shedding frequency [Hz]	400.2	781.9	1123.6	1378.8

The results from the modal analysis of guide vanes 3316, 3318 and 3320 both in air and when submerged in water are summarised in table 4.

Table 4. Numerically obtained natural frequencies of guide vanes 3316, 3318 and 3320 in air and in water.

	3316		**3318**		**3320**	
	Natural Frequency					
Mode	in Air [Hz]	in Water [Hz]	in Air [Hz]	in Water [Hz]	in Air [Hz]	in Water [Hz]
1	2964.7	1850.3	2928.6	1930.1	2925.3	1992.3
2	5231.8	3123.1	5529.4	3286.6	5779.4	3399
3	7376.5	5376.8	8149.7	5938.9	8755.3	5873.5
4	10606	6123.8	10873	6119.5	10720	6669.6
5	11419	7895.6	10980	8563.7	10726	8895.5
6	11475	9006.5	11374	9646.3	11796	10070

The six mode shapes of the guide vanes are presented on figure 9.

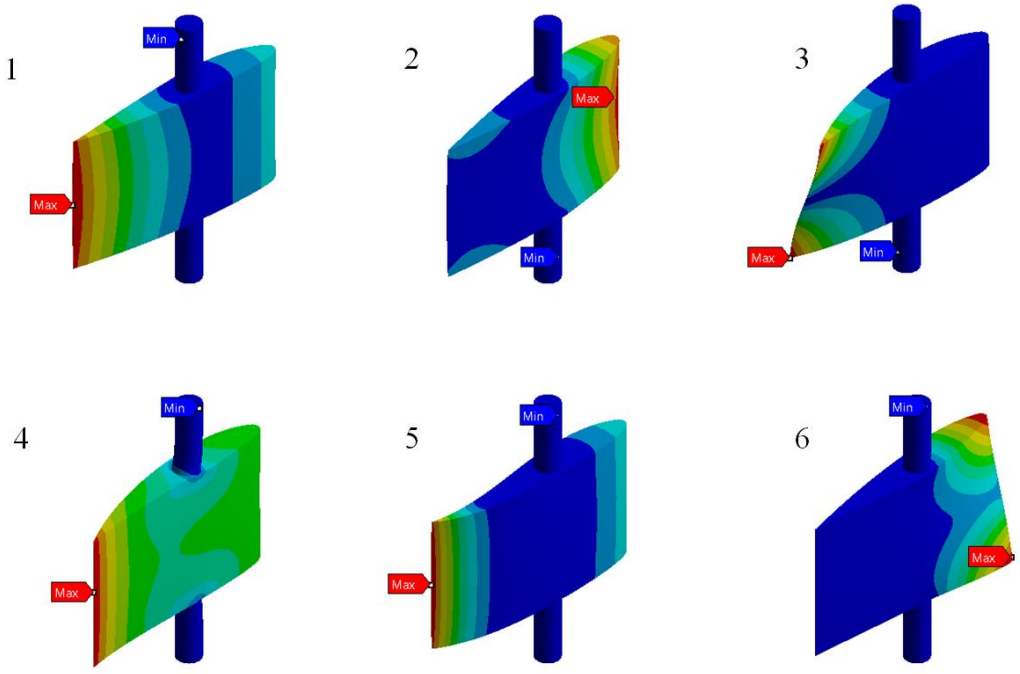

Figure 9. Guide vane 3316 mode shapes

From the vortex shedding and blade passing frequency calculations and the numerical results for guide vanes natural frequencies, it can be observed that the natural frequency of each guide vane is closest to the value of vortex shedding frequency at high load, but far enough not to face the risk of resonance. The comparison is given in table 5.

Table 5. Obtained natural frequencies and vortex shedding frequencies for guide vanes 3316, 3318 and 3320.

	Natural frequency in 1st mode [Hz]	Vortex shedding frequency at high load [Hz]
3316	1850.3	1378.8
3318	1930.1	1379.5
3320	1992.3	1378.7

5. Conclusions

In this paper, the stress parameters of three modifications of Francis turbine guide vanes were analysed, named NACA 3316, NACA 3318 and NACA 3320, since they are derived using the analytical equations of 4 digit NACA airfoils. Steady state CFD simulations in ANSYS CFX are performed in order to obtain the pressure field of the guide vanes cascade. The pressure distribution is applied to the guide vanes surfaces of the finite element model (one-way FSI). Stress distribution and deformation of guide vanes were analysed to gain an understanding of the influence of both the profile thickness and the operating regime.

It was concluded that the total deformation decreases with the thickness of the guide vane for the same operating regime. Moreover, the deformation increases when going from high load to deep part load for every type of guide vane. Regarding stress, it was observed that it increases going from high load to deep part load operation for every type of profile. The highest value of Von-Mises stress was noticed for guide vane 3318 at deep part load operation.

Natural frequencies of the guide vanes were numerically obtained considering the added mass effect of the surrounding water. In addition, the blade passing frequency was calculated and the vortex shedding frequencies for all cases were obtained.

It was observed that the excitation frequencies are slightly lower than the guide vanes' natural frequencies, which gives possibility of further reduction of the airfoil thickness.

References

[1] Flores M, Urguiza G and Rodriguez J M 2012 A fatigue analysis of a hydraulic Francis turbine runner *World Journal of Mechanics* **2** (1)
[2] Valentin D, Presas A, Bossio M, Egusguiza M, Egusguiza E and Valero C 2018 Feasibility of detecting natural frequencies of hydraulic turbines while in operation, using strain gauges, *Sensors* **18** (1) 174
[3] Hau E 2000 *Wind turbines: Fundamentals, Technologies, Application and Economics* Springer
[4] Tartibu L 2008 *A simplified analysis of the vibration of variable length blade as might be used in wind turbine systems*, Thesis
[5] Knight C E 1993 *The Finite Element Method in Mechanical Design*, PWS-Kent publishing company
[6] Hengstler Johannes A N 2013 *Influence of the Fluid-Structure Interaction on the Vibrations of Structures*, Doctoral thesis
[7] Roth S Hasmatuchi V Botero F Farhat M and Avellan F 2010 Fluid structure coupling in the guide vanes cascade of a pump-turbine scale model *IOP Conf Series: Earth and*

Environmental Science **12**
[8] Hallen M J S 2018 *Simulation of rotor-stator interactions (RSI's) in a high head Francis turbine*, Master thesis
[9] Magnoli M V and Maiwald M 2014 Influence of hydraulic design on stability and on pressure pulsations in Francis turbines at overload, part load and deep part load based on numerical simulations and experimental model test results *IOP Conf Series: Earth and Environmental Science* **22**
[10] Agnalt E Iliev I Solemslie B W and Dahlhaug O G 2019 On the rotor-stator interaction effects of low specific speed francis turbines *Int J. Rotating Mach.*
[11] Guillame R Deniau J L Scolaro D and Colombet C 2012 Influence of the rotor-stator interaction on the dynamic stresses of Francis runners *IOP Conf Series: Earth and Environmental Science* **15**
[12] Ostby T K Petter Myrvold E Billdal J T and Haugen B 2019 Excitation of torsional modes in guide vanes *IOP Conf Series: Earth and Environmental Science* **240**
[13] Seidel U Hubner B Lofflad J and Faigle P 2012 Evaluation of RSI induced stresses in Francis runners *IOP Conf Series: Earth and Environmental Science* **15**
[14] Strouhal V 1878 On an unusual sort of sound excitation *Annalen der Physik und Chemie* **5** (10) 216-251
[15] White M Frank 1999 *Fluid Mechanics*, McGraw Hill
[16] Neidhardt T Jung A Hyneck S and Gummer J 2018 An alternative approach to the Von Karman vortex problem in modern hydraulic turbines *The International Journal on Hydropower and Dams* **25** (3)
[17] https://www.simulation-conference.com/library/r%C3%BCckblick_2014/Submit_Huebner_ACUM_2014.pdf
[18] Liang Q W Rodriguez C G Egusguiza E Escaler X Farhat M and Avellan F 2007 Numerical simulation of fluid added mass effect on a Francis turbine runner, *Computational Fluids* **36** 1106-1118
[19] Egusguiza E Valero C Liang Q Coussirat M and Seidel U 2009 Fluid added mass effect in the modal response of a pump-turbine impeller *Proc. of the ASME 2009 International Design Engineering Technical Conferences and Computers and Information in Engineering Conf* San Diego 715-724
[20] Bossio M Valentin D Presas A Martin D R Egusguiza E Valero C Egusguiza M 2017 Numerical study on the influence of acoustic natural frequencies on the dynamic behavior of submerged and confined disk-like structures *J. Fluids Struct.* **73** 53-69
[21] https://www.ntnu.edu/nvks/f99-test-case1
[22] https://www.ntnu.edu/nvks/f99-test-case2

Acknowledgements

This research was supported by the European's Union Horizon 2020 project HydroFlex.
We used the test-case provided by NTNU-Norwegian University of Science and Technology under the Francis-99 workshop series.

This project has received funding from the European Union's Horizon 2020 research and innovation programme under grant agreement No 764001

HydroFlex